

Problems of modeling the creation the surface laser-induced structures in relaxed optics

P. P. Trokhimchuck

Lesya Ukrayinka East European National University,

Voly av. 13, Lutsk, Ukraine, 43025

Experimental data of formation laser-induced surface structures on silicon, germanium and titanium are represented. Problems of modeling the creation the surface laser-induced micro and nanostructures are observed. Comparative analysis of plasmic, synergetic (theory of Benar phenomenon) and physical-chemical methods (cascade model of excitation the proper chemical bonds in the regime of saturation the excitation) are represented and discussed. These methods were used for modeling the processes of creation surface laser-induced structures in silicon, germanium and titanium. Cascade model explanation these experimental data is more full and really as other models.

Keywords: laser irradiation; surface structures; Benar phenomenon; cascade model; relaxed optics.

Наведені експериментальні результати утворення лазерно-індукованих поверхневих структур на кремнії, германії та титані. Досліджуються проблеми моделювання утворення поверхневих лазерно-індукованих мікро та наноструктур в релаксаційній оптиці. Проведено порівняльний аналіз та обговорення плазмових, синергетичних (теорія ефекту Бенара) та фізико-хімічних методів (каскадна модель збудження відповідних хімічних зв'язків в режимі насичення збудження). Ці методи були апробовані для пояснення процесів утворення поверхневих лазерно-індукованих структур на кремнії, германії та титані. Каскадна модель в порівнянні з іншими дозволяє більш повно та адекватно пояснити наведені експериментальні результати.

Ключові слова: лазерне опромінення, поверхневі структури, явище Бенара, каскадна модель, релаксаційна оптика.

Приведены экспериментальные результаты по образованию лазерно-индуцируемых поверхностных структур на кремнии, германии и титане. Исследуются проблемы моделирования образования поверхностных лазерно-индуцируемых микро и наноструктур в релаксационной оптике. Проведен сравнительный анализ и обсуждение плазменных, синергетических (теория эффекта Бенара) и физико-химических методов (каскадная модель возбуждения соответствующих химических связей в режиме насыщения возбуждения). Эти методы были апробованы для объяснения процессов образования поверхностных лазерно-индуцируемых структур на кремнии, германии и титане. Каскадная модель в сравнении с другими позволяет более полно и адекватно объяснить данные экспериментальные результаты.

Ключевые слова: лазерное облучение; поверхностные структуры; явление Бенара; каскадная модель; релаксационная оптика.

Introduction

Problems of modeling the creation the surface laser-induced micro and nanostructures is very interesting. We can have various processes and phenomena, which are connected with photochemical, plasmic and thermochemical processes [1]. As rule it is the cascade and circle processes. Irreversible changes of laser-irradiated surface of matter must be explained as phase transformations.

So, the laser-induced transition in Ge from cubic (diamond) to hexagonal symmetry was represented as Benar phenomena in solid [2]. But Benar phenomenon is caused of the transition from heat conductivity to convection in liquid [3 – 6]. This hexagonal phase is two-dimensional. But the laser-induced structures have

three-dimensional crystal nature. Therefore cascade model (CM) of step-by-step excitation of chemical bonds in the regime of saturation the excitation allow explaining these experimental data more adequate as modified Chandrasekar-Haken-Ebeling [3 – 5] or Kolmogorov-Petrovskiy-Piskunov [6] theories of Benar phenomena.

A suitability of application CM is caused the large dispersion of heights of laser-induced surface structures: from 10-15 nm for Nd-laser irradiation of Si and GaAs [2] to 20-50 μm for multipulse nanosecond eximer KrF-laser irradiation of Si (wavelength 248 nm, pulse duration 25 ns, 1500 – 2000 pulses) [7, 8]. Only phase transitions from diamond symmetry (initial matter) to structures with more low symmetry (hexagonal, triclinic or monoclinic)

allow receiving the last results. Estimation of regimes of irradiation [7, 8] shows the possibility of these processes. Thus we can have multiphase structure from ground of our microcolumn to his peak. More low symmetrical structures are generated in the upper part of laser-induced microcolumn. Practically we have laser-induced swelling or surface ionizing blistering of silicon. But for case of change crystal symmetry this swelling has more large height. The creation only one phase (Ge irradiation by 15 ns pulses of Nd-laser, ~ 20 – 50 pulses) with change crystal symmetry from diamond to hexagonal allow to receive 200 nm nanohills [2]. The environment practically isn't influence on the geometrical sizes (heights) of created laser-induced surface nano and micro structures [2, 7, 8, 10].

CM may be used too for the explanation the laser-induced redistribution (interferograms) on titanium [9]. Titanium has two phases: low temperature hexagonal α -Ti and high temperature cubic β -Ti. We have only cubic phase for titanium heating more as $882,5^\circ C$ [11]. But laser irradiation allows separating these phases. In the peaks of interferograms we must have hexagonal Ti (may be other as α -Ti) and in the ground of interfertograms we must have cubic titanium (may be other as β -Ti). This redistribution is caused of electronegativity conditions of this phases and its geometrical volume.

Experimental data

First experimental data of irreversible interaction the laser radiation and semiconductors were received by M. Birnbaum in 1965 [12]. He observed the surface interferograms after pulse Ruby-laser irradiation of germanium (Fig. 1), silicon, indium antimonite a.o. [12]

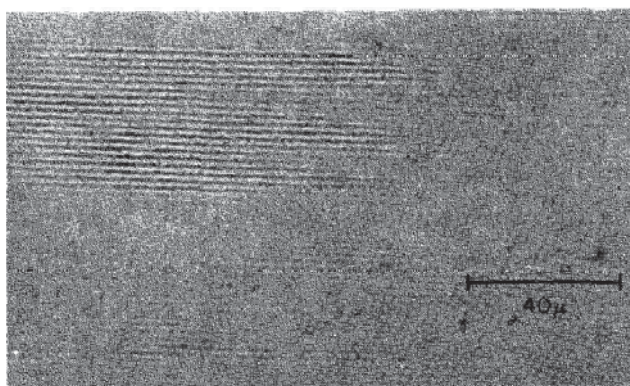


Fig. 1. Photomicrograph of Ruby laser induced surface damage of {100} face of a germanium sample [12].

Later these results were developed to interference laser annealing of semiconductors [1]. But this fact is corresponded to the structural changes of laser-irradiated pure matter and matter with impurity and damages. Impurities and damages in the irradiated material have little influence on the formation of the interferograms [1, 10]. Nanostructures formed by crest of interferograms. Its formation is depended from parameters of irradiation.

Therefore these phenomena have more deep nature as laser annealing of ion-implanted materials [1].

Surfaces nanostructures were received after irradiation of SiO_2/Si structure by second harmonic Nd:YAG laser at density of power $I=2.0 MW/cm^2$, pulse duration 10 ns, wavelength 532 nm and frequency of repetition 12,5 Hz (Fig. 2.) [2].

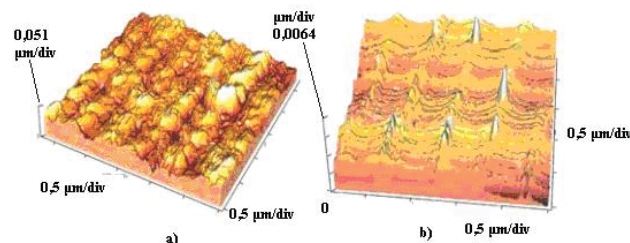


Fig. 2. AFM 3D images of: (a) SiO_2 surface after irradiation of SiO_2/Si structure by second harmonic Nd:YAG laser at $I=2.0 MW/cm^2$ and (b) Si surface after subsequent removing of SiO_2 by HF acid [2].

More detail research of creation the surface laser-induced structures are represented by A. Medvids in [2]. Samples of Ge {111} and Ge {001} i-type single crystals are used in experiment. Nd:YAG laser (wavelength 1,064 μm , duration of pulse 15 ns, pulse rate 12,5 Hz, power $P=1 MW$) was used for the irradiation.

The AFM picture of Ge surface after Nd laser irradiation is represented in Fig. 3 [12].

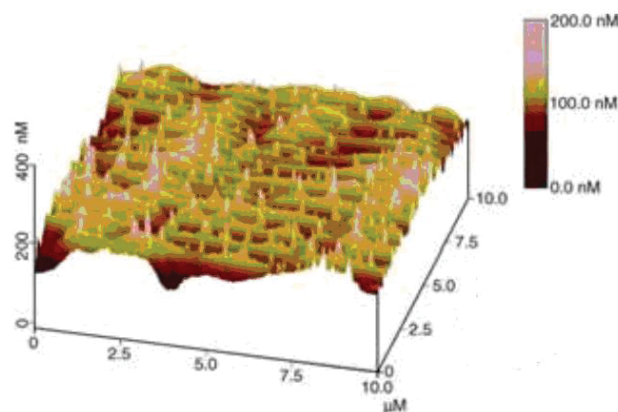


Fig. 3. Three-dimensional AFM image of nanostructures after Nd:YAG laser irradiation with density of power 28 MW/cm^2 on Ge surface [12].

More large columns (height 20 μm , diameter 2 – 3 μm) were received after irradiation of pulse series the nanosecond eximer KrF-laser (wavelength 248 nm, pulse duration 25 ns) (Fig. 4). This figure illustrates the high aspect ratio silicon micro-columns that were formed in air after 1000 laser shots at an energy density, E_d , between 2.7 and 3.3 J/cm^2 . The columns are ~20 μm long and ~2~3 μm in diameter. Moreover, surface-height profilometry performed using a Dektak II profiler revealed that most

of the length of the microcolumns, 10 – 15 μm , protrudes above the original Si surface [7].

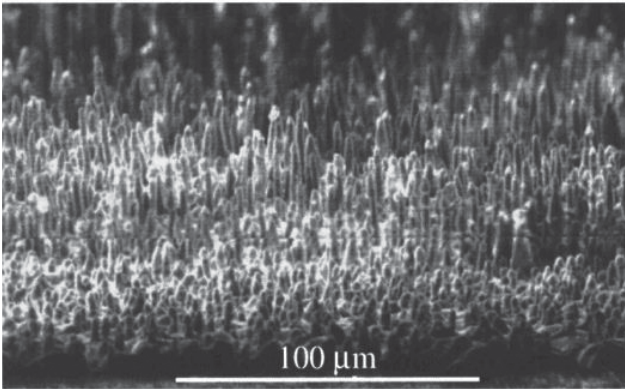


Fig. 4. SEM images of silicon nanocolumns after 1000 laser shots in air at $E_d = 3 \text{ J/cm}^2$ [7].

The microcolumn morphology changes if the atmosphere is changed during laser irradiation. Fig. 5 shows several columns in a specimen that was first irradiated with 600 pulses in air and 1200 pulses in $\text{N}_2/5\% \text{O}_2$ [7].

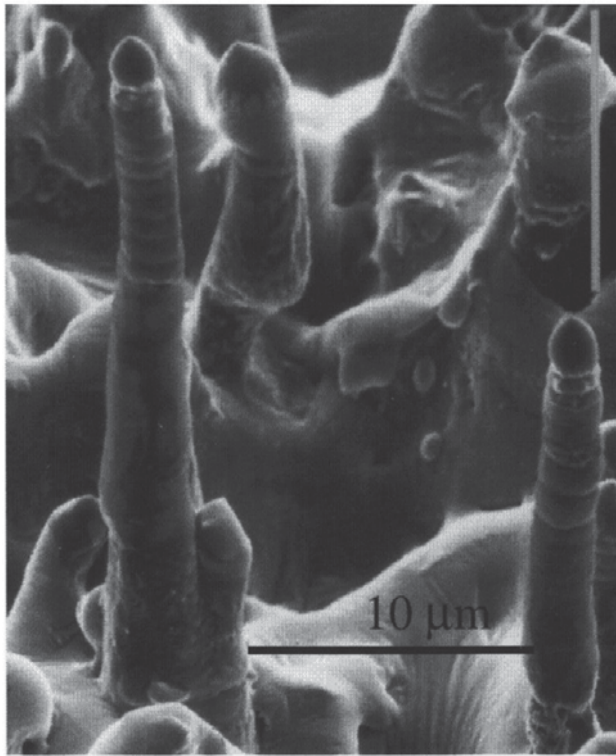


Fig. 5. SEM image showing a change in Si microcolumn morphology controlled by the ambient gas composition at $E_d 2.7 \text{ J/cm}^2$. The arrows indicate the height achieved after 600 laser pulses in air ($\text{N}_2 - 18\% \text{O}_2$); the remainder of the columns was grown by 1200 laser pulses in $\text{N}_2 - 5\% \text{O}_2$ [7]

The importance of the gas environment was emphasized, when a plasma etchant, SF_6 , was used as the ambient gas during laser irradiation of silicon [7]. In SF_6 extremely long structures are produced that look at first like walls surrounding very deep central holes (see Fig.6) [7].

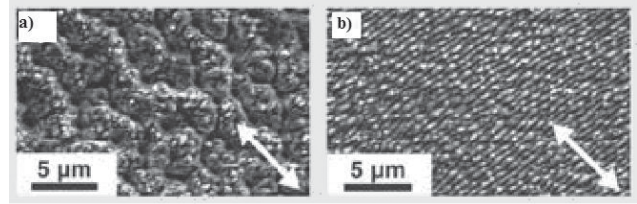


Fig. 6. Walled Si structure produced by 2040 laser pulses at $E_d = 1.5 \text{ J/cm}^2$ in 1 atm of SF_6 [7].

Ordered laser-induced nanostructures, which were created on surface of Si after laser irradiation ($\lambda = 0,8 \mu\text{m}$, $\tau_i = 100 \text{ fs}$, number of pulses 200) through lay of water, are represented on Fig. 7. Three types of micro and nanostructures are generated [10, 13]. Nanostructures have typical spatial scale $d_1 = 600 \text{ nm}$ and $d_2 = 120 \text{ nm}$, here lattice vector oriented $\vec{g} \parallel \vec{E}$. It is corresponded to interference between surface polariton-plasmon (SPP) and TM electromagnetic wave. Structures with period d_1 are generated for interference of falling wave with SPP wave, which arise on the border water – free electrons of silicon. Structures with period d_2 are generated for mutual interference of two SPP, which were propagated in mutually inverse directions along border silicon – plasmonic layer. Structures with period 120 nm aren't depended from nature of liquid, which was contacted with silicon [10]. It is experimental fact.

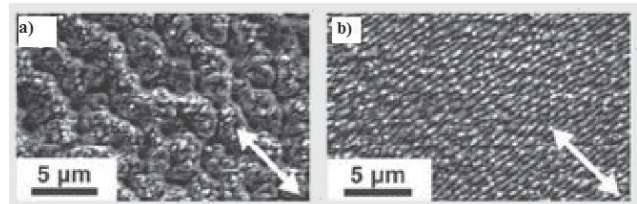


Fig. 7. Ordered structures, which were generated on surface of silicon after laser irradiation through lay of water, (arrow in lower angle show the direction of polarization of laser radiation); duration of pulse 100 fs , wavelength – 800 nm , number of pulses 200, density of energy the irradiation a) 25 kJ/m^2 , b) 5 kJ/m^2 [13].

Laser-induced silicon nanostructures ($\lambda = 0,8 \mu\text{m}$, $\tau_i = 100 \text{ fs}$, number of pulses 200) with $d_3 = 90 \text{ nm}$, which was generated after irradiation structures of changing polarization with $d_2 = 120 \text{ nm}$, when orientation of vector \vec{E} was changed on 90° relatively to initial action. Power of laser irradiation was less in two time as for initial structure. Generated periodical structures (Fig. 8 and Fig. 9 are nanocolumns with height to 400 nm with spatial period 90 nm and orientation wave vector $\vec{g} \parallel \vec{E}$. [10, 13]. Where \vec{g} is beam propagation direction.

Generation of periodical nanostructures along crests ($d = 90 \text{ nm}$) is cause with interference of falling radiation with surface polaritons, which are exited along crest of relief ($d \sim 120 \text{ nm}$), and with mutual interference of surface polariton-plasmons [10]. A crest of relief, which considered

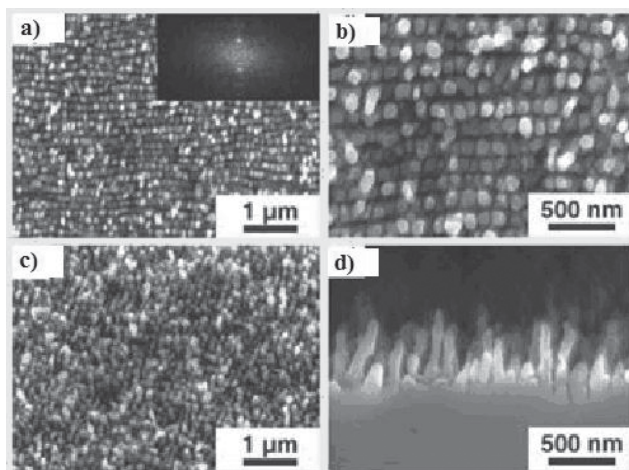


Fig. 8. Nanocolumns, which are generated after irradiation structures of silicon with $d_2=120$ nm, (wavelength of irradiation 800 nm, number of pulses – 200, density of energy of irradiation $0,5$ kJ/m²): a) and b) turn of polarization on 90°, c) turn of polarization on 45°, d) cross chip of nanocolumns. On insertion to Fig. 8a – Fourier-picture of structures [13].

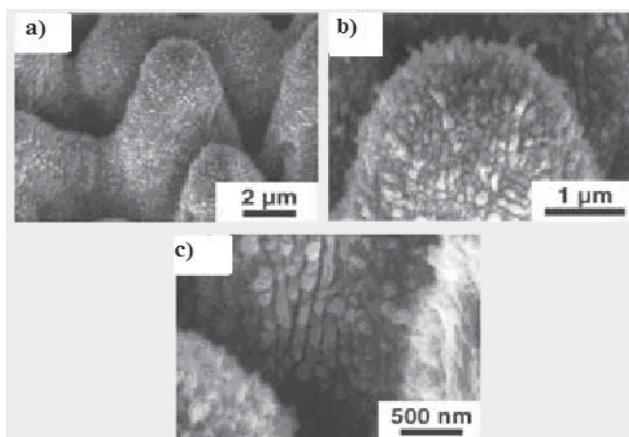


Fig. 9. Surface silicon nanocolumns of little scale, which have orthogonal orientation to a crests of nanorelief of large scale [13].

in contact with the substrate, was selected as initial half-cylinder. Formed in this case inoculating regular relief $d \sim 90$ nm is basis for further growth of nanocolumns. Since typical radius of half-cylinder $r \ll \lambda$ therefore dispersion relation for surface polariton-plasmon in cylindrical geometry is changed from dispersion relation in plane geometry of phase separation. It cause to formation nanostructures with less period as for plane case [10].

For case of elliptic polarization and falling angle to surface from 0 to 20° basic nanostructures are created: 1) surface nanostructures with period ~ 200 nm and 2) these structure with period 70–100 nm are generated on crest of structure 1, but its orientation $\vec{g} \perp \vec{E}$ [10].

Basic difference between nanosecond (Fig. 2, Fig.4 – Fig. 6) and femtosecond regimes of creation of surface silicon nanostructures (Fig. 7 – Fig. 9) is the its sizes: 15–20 nm for nanosecond regime of irradiation (nanohills)

for Neodimium laser (Fig. 2), 20 – 50 μm for eximer laser (Fig.4 – Fig.6) and 400–450 nm for femtosecond regime of irradiation (Fig.7 – Fig.9). These data are proved electromagnetic mechanisms of creation surface nanostructures (surplus of negative charge is caused the electromagnetic swelling of surface) [1, 10, 14]. Heat processes are caused the decrease of sizes, including height of surface nanostructures. But we have nanosecond laser-generated silicon microstructures (Fig. 4 – Fig. 6) and 200 nm germanium microstructures (Fig. 2), which are shown an influence of intensity and mechanisms of light absorption and number of pulses on the generation surface structures.

For the modeling processes of Fig. 7 we must develop electromagnetic concept of RO. This concept allows including in parametric optical processes back side of “medal”: resulting trace of interaction light and matter in matter [1, 14].

An influence of pulses number on the processes of formation of laser-induced periodic nanostructures on titanium plate is observed in [9]. Sapphire laser system was used for the irradiation. It had next parameters: wavelength 800 nm, repetition rate 1 kHz, pulse length 100 fs, beam diameter 4 mm and density of energy of irradiation 0,25; 0,75 and 1,5 J/cm². Interference structures are generated for the irradiation with energy density 0,25 J/cm² [9]. Evolution of creation laser-induced surface structures are represented in Fig. 10.

The period of the parallel periodic microstructures as a function of the number of laser pulses is shown in Fig. 11 [9].

As shown in Fig. 11, the period was gradually increased in the range of 10–70 pulses and increased in the range of 70–110 pulses as the number of pulse increased.

Distance between the microdots along the hill of periodic microstructures as a function of the number of laser pulses is shown in Fig. 12 [9]. As Fig. 12 shows, the distance was increased in the range of 50–110 pulses. But these distances are correlated with height and width of interference bands (Fig. 10).

Phenomenon of doubling of period of laser-induced surface structures is represented in Fig. 13 [9].

Modeling and discussions

Therefore we must estimate all possible mechanisms of relaxation: kinetic and dynamical; and possible mechanisms of excitation: hierarchical photo ionization. In this case we must include respective chain of relaxation times [1]. It is necessity for the more full representation and modeling real and possible physical processes for the respective regimes of interaction.

Thus this representation of the modeling dangling bonds, which are created with help laser irradiation, is very effective method. It allows including in consideration

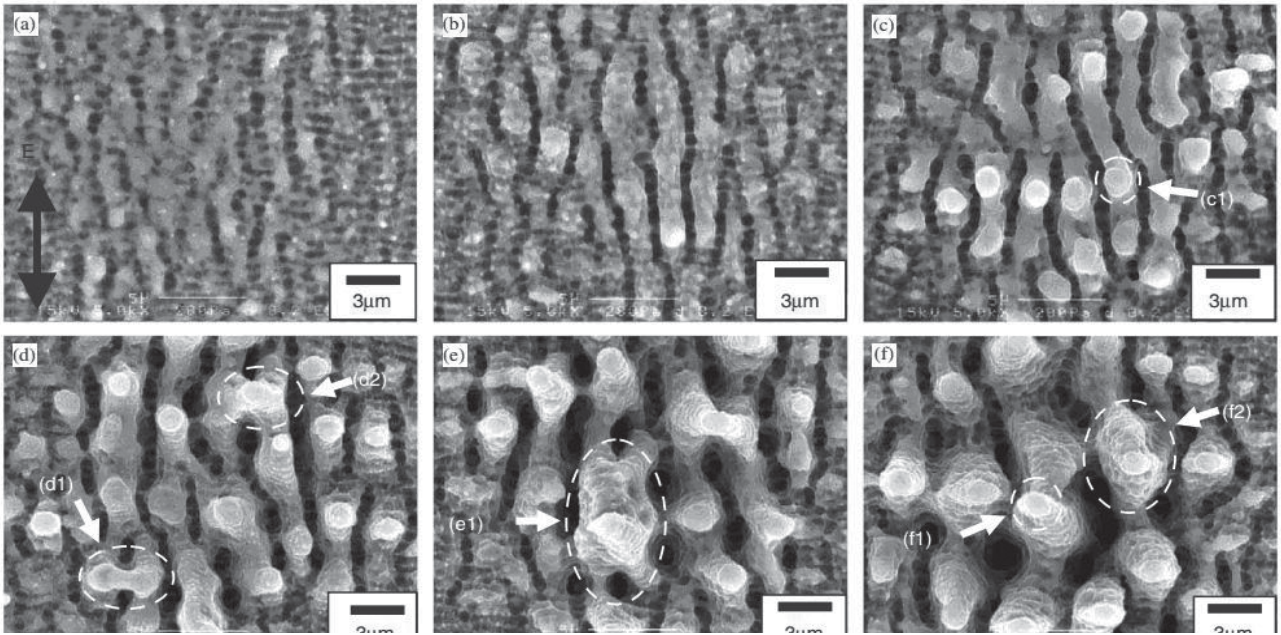


Fig. 10. Microstructures produced on the titanium plate at the laser fluence of 0.75 J/cm^2 for (a) 10, (b) 25, (c) 50, (d) 70, (e) 90 and (f) 110 pulses [9].

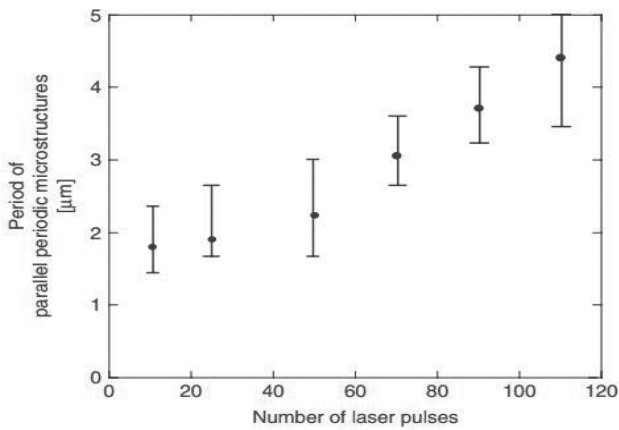


Fig. 11. Period of parallel periodic microstructures as a function of number of laser pulses [9].

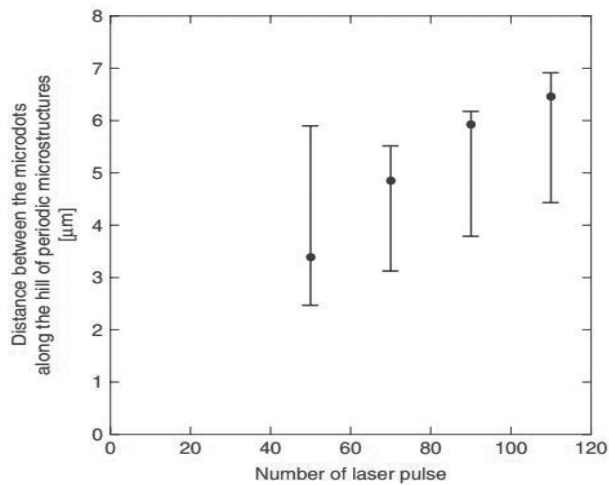


Fig. 12. Distance between the microdots along the hill of periodic microstructures as a function of the number of laser pulses [30].

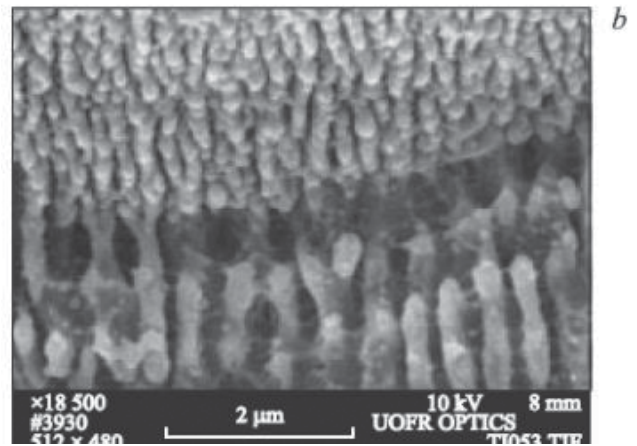
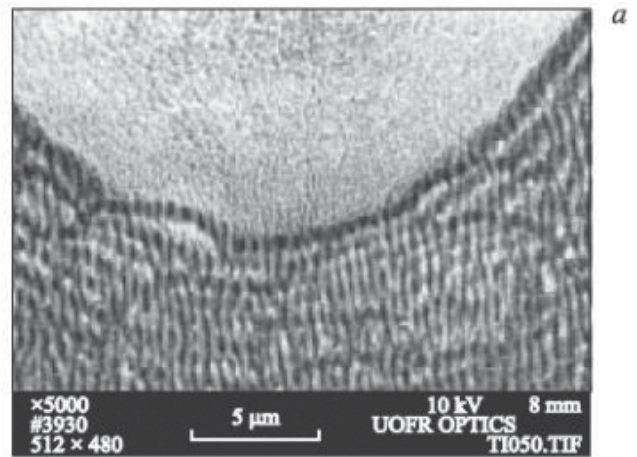


Fig. 13. Relief of Ti surface after pulse linear polarized laser irradiation (power density $1,1 \text{ GW/cm}^2$, number of pulses – 100): period of structures – 600 nm, b) region of transition from structures with period 600 nm to period 300 nm [9].

effects of equilibrium, nonequilibrium and irreversible relaxations [1].

Now we show the using of cascade model for the explanation experimental data of laser-induced phase transformations in silicon, germanium, carbon and titanium. It was called as case the structural phases.

The question about the influence of saturation of excitation on effects of RO may be represented as process of transitions between stable and metastable phases too. Now we'll estimate the influence of parameters of irradiation (including spectral) on irreversible changes and transformations in *Si* and *Ge*. Spectral dependences of absorbance of various structural modification of Si are represented on Fig.14 [1, 15]. Now we'll be estimated intensities of eximer, Ruby and Neodymium laser irradiation (wavelengths of irradiation are 0,248 μm , 0,69 μm and 1,06 μm properly of silicon and germanium, which are necessary for the creation of proper irreversible changes in irradiated semiconductor. As shown in [16], absorbance of the Neodymium laser radiation in silicon is equaled 100 cm^{-1} , second harmonic of Neodymium laser – 10⁴ cm^{-1} , eximer laser – 10⁶ cm^{-1} .

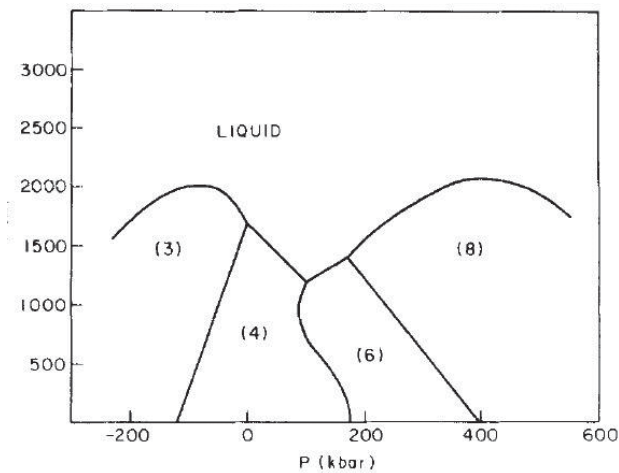


Fig. 14. A schematic phase diagram for *Si*(CN). The coordination numbers (CN) of the various phases are indicated. The diagram is based on common features of the phase diagrams of column IV elements as described by the references cited in Pistorius's review (Ref. 8 in [15]). Starting from a high temperature $>3 \times 10^3 \text{K}$ and subject to a constraint of average density $\langle \rho \rangle = \rho(4)$, a hot micronucleus will tend to bifurcate into the most stable phases (highest T_m) which straddle *Si*(4) in density. These are *Si*(3) and *Si*(8), as indicated by the diagram [15].

Crystal semiconductors Si and Ge have, basically, the structure of diamond. Volume atomic density of elementary lattices may estimate according to formula [1]

$$N_a = \frac{\rho N_A}{A}, \quad (1)$$

where ρ – density of semiconductor, N_A – Avogadro number, A – a weight of one gram-atom. For *Si* $N_{aSi} = 5 \cdot 10^{22} \text{ cm}^{-3}$ and for *Ge* $N_{aGe} = 4,4 \cdot 10^{22} \text{ cm}^{-3}$.

But Si and Ge may be crystallized in lattices with hexagonal, cubic, trigonal and monoclinic symmetry. Phase diagram of Si as function of coordination number is represented on Fig. 14.

Coordination number (CN) 8 is corresponded of diamond lattice, CN 6 – hexagonal lattice, CN 4 and CN 3 – other two lattices. It should be noted that melting temperatures of these phases are various. Volume density of CN is equaled $\text{CN} \cdot N_a$. For diamond symmetry of lattice this value is $8N_a$.

Roughly speaking, transition from one phase to another for regime of saturation of excitation may be modeled as one-time breakage of proper numbers of chemical bonds, which are corresponded to the difference of CN of proper phases. For example, two bonds breakage is caused the phase transition from diamond to hexagonal structure. One bond breakage in the regime of saturation is caused to generation of laser radiation.

Results of calculation of volume densities of energy, which are necessary for breakage of proper number of bonds in regime of saturation of excitation, are represented in Table 1. It conceded that energies of all chemical bonds for elementary lattice are equivalent (*Si* and *Ge* are pure homeopolar semiconductors) [1]. For silicon energy of covalent bonds *Si-Si* are equaled 1,2–1,8 eV; for germanium energy of covalent bonds *Ge-Ge* are equaled 0,9–1,6 eV. Minimal values of these energies are corresponded of Pauling estimations. These values are corresponded the energy on one CN: according to radiation physics of status solid Zeits energy of creation one radiation defect is equal 12,7 eV for diamond lattice [17].

Table 1.

Volume density of energy I_v (10^3 J/cm^3), which is necessary for the breakage of proper number of chemical bonds in the regime of saturation of excitation in *Si* and *Ge*.

	I_{v1}	I_{v2}	I_{v4}	I_{v5}
Si	12,8–14,4	25,6–28,8	51,2–57,6	63–72
Ge	6,3–8,4	12,6–16,8	25,2–33,6	31,5–42

Surface density of energy on proper numbers of CN for proper lasers irradiation may receive after division of results of Table 1 on proper absorbance. This procedure allows to transit from bulk to surface density of energy, which is necessary for the receiving of proper phenomena. Results of these calculations are represented in Table 6.

It should be noted that real regimes of irradiation must be more (process of light reflection wasn't included in our estimations). In addition we aren't include the relaxation (time) processes for the scattering of light on stable centers (self-absorption in crystals) as for InSb and InAs [1].

Table 2.

Surface density of energy I_{si} (J/cm²), which are necessary for the breakage of proper numbers of chemical bonds in Si and Ge crystals after proper lasers irradiation in regime of saturation the excitation [1, 2, 4]

	I_{s1}	I_{s2}	I_{s4}	I_{s5}
Si, 1,06 μm	128 – 144	256 – 288	512 – 576	630 – 720
Si, 0,53 μm	1,28 – 1,44	2,56 – 2,88	5,12 – 5,76	6,3 – 7,2
Si, 0,248 μm	0,0128 – 0,0144	0,0256 – 0,0288	0,0512 – 0,0576	0,063 – 0,072
Ge, 1,06 μm	0,63 – 0,84	1,26 – 1,68	2,52 – 3,36	3,15 – 4,2
Ge, 0,53 μm	0,32 – 0,42	0,63 – 0,84	1,26 – 1,68	1,58 – 2,1

Remark to Table 2: absorbcencies of *Si* (Neodimium laser) – 100 cm⁻¹; *Si* (second harmonic of Neodimium laser) – ·10⁴ cm⁻¹; *Si* (eximer laser) – ·10⁶ cm⁻¹. *Ge* (Neodimium laser) – ·10⁴ cm⁻¹; *Ge* (second harmonic of Neodimium laser) – 2·10⁴ cm⁻¹.

Height of surface nanostructures for the nanosecond regime of irradiation is maximal (200 nm, Fig.2) for the germanium [2] for small number of pulses and for silicon (20 – 50 μm, Fig. 4 – Fig. 6) for large number of pulses [7,8]. For the silicon (Fig. 2) height of laser-generated surface nanostructures is change from 10 nm to 20 nm. This difference can be explained in next way. Index of light absorption with wavelength 532 nm of Ge crystal with diamond symmetry is more as silicon with this symmetry for the nanosecond irradiation. But surface part of irradiated germanium is transited to hexagonal phase. It is experimental data. Other result given's phase transitions. The hexagonal lattice of germanium has greater size as diamond modification. Therefore hexagonal nanostructures are greater and more stable as polycrystalline or metallic nanohills.

Mechanisms of creation other laser-induced nanostructures may be explained on the basis cascade model of step-by-step excitation of corresponding type and number of chemical bonds in the regime of saturation of excitation. According to this model decrease of symmetry of irradiated matter is occurred with increase of intensity of irradiation (Nd laser irradiation of silicon, germanium and carbon) [1].

But in [2] the explanation of creation laser-induced hexagonal phase on germanium surface is based on the Benar phenomenon: generation of hexagonal phases in heated liquid on roaster. This effect is observed for few liquids. Chandrasekar theory is described this process as thermal-diffusive processes [3 – 5]. In this case we have transition from more low volume symmetry to more high surface symmetry. Chandrasekar created the hydromagnetic theory of creation sunspots [4].

For laser-induced creation volume hexagonal structures on *Ge* we have inverse transition: from high volume symmetry (diamond modification) to more volume low symmetry (hexagonal symmetry) [2].

Now we represented estimations of process the creation laser-induced hexagonal structure on the basis Chandrasekar-Haken theory [4] and cascade model [4].

Creation of instability is characterized of critical point. This point my be characterized by Rayleygh anf Nusselt numbers [4].

Rayleygh number is determined as

$$Ra = \frac{g\alpha\beta}{\kappa\nu} h^4, \quad (2)$$

where g – free fall acceleration, α coefficient of volumetric expansion, $\beta = \frac{\Delta T}{h}$ – temperature gradient,

κ – coefficient of heat conductivity, ν – kinematic viscosity, h – thin of heated films.

Nusselt number determined as

$$Nu = \frac{|q|h}{\kappa_0\Delta T} = \frac{|q|}{\beta\kappa_0}, \quad (3)$$

where κ_0 – statistical value of coefficient of heat conductivity, q – full heat flow.

$N_u = 1$ for case of heat transfer only with help heat conductivity and $N_u > 1$ for case of heat transfer with help heat conductivity and convection. Behavior function $Ra(N_u)$ in critical point is analogous to curve of phase transition.

Critical value Rayleygh number is equaled $Ra_{crit} = 1700 \pm 51$. For $Ra > Ra_{crit}$ and $N_u > 1$. For regime of irradiation of Fig. 2 $Ra < 1$ and $N_u < 1$ Therefore application this theory to these results is very ambiquous and discussed.

According by Haken probability of creation hexagonal structures is major for $Ra \geq Ra_{crit}$. For further increasing of Rayleygh number a generation of cylindrical structures is basic. It explains of occurrence the curls in atmosphere [3].

But conditions of creation new phases in solid phase is other as in liquid phase. Chandrasekar – Haken theory may be used for the modeling processes of growth $Si_{1-x}Ge_x$ whiskers with diameter $> 40 \mu m$ [18]. These crystals have hexagonal cross-section. Basic methods of receiving these structures are thermal (epitaxial and sputtering, including

laser ablation)). For decreasing sizes to 1 μm we have circular cross-section [18] and properties of whispers is identical to bulk matter. For case of laser implantation we must include chain electromagnetic processes of creation vortexes (nanohills and nanocolumns or according by Makin polariton-plasmons) and chain photochemical processes, which are connected with intensive photo ionization of irradiated layers. These surface polariton-plasmons may be having various electromagnetic structures. They are having transverse or longitudinal polarization [10].

The influence of pulse numbers on generated the surface interferograms on titanium was received in [7, 8] (Fig. 10 – Fig. 12). For explanation these results may be used the cascade model of saturation the excitation. Irradiated titanium has two phases: α-phase (hexagonal) and β-phase (body-centered cubic lattice). Temperature of phase transition α → β is equaled 882,5°C [11]. Hexagonal structure has more large electronegativity, therefore the interference maximum of Fig. 10 must be have α-symmetry. Increasing of number pulses is caused of saturation the interference band and generation nano and microstructures.

The mechanisms of light absorption are influenced on the relaxation time of excitation. Proper phenomenological chain of relaxation times is represented in [1]. The number of disrupt chemical bonds or CN may be determined with help next formula

$$n = 2 \ln \frac{h\nu}{E_a} . \quad (4)$$

Where E_a – the energy of ionization (breakage) of proper bond.

More pure ionizing results were received for the irradiation silicon by femtosecond laser pulses in multipulse regime [13]. One quantum of eximer laser radiation may be ionized 3,5 chemical bonds according to formula (4). Therefore multipulse regime of the irradiation is caused the generation silicon structures with hexagonal and trigonal symmetry. Density of energy 2,7 J/cm² (Fig.5) and 1,5 J/cm² (Fig. 6) certificated this hypothesis according to Table 2. First regime (Fig. 5) allows receiving more thin and high structures with more low symmetry, which is stipulated more high intensity of irradiation. Second regime (Fig. 6) may be results of generation the structures with more low symmetry (no cubic). Atmosphere of irradiation must be has neglected influence on finishing picture. This conclusion is certificated by experimental data of Fig. 7 – Fig. 9.

For light absorption on unstable centers (amorphous semiconductors) time characteristics haven't large observable influence on formation of irreversible changes in semiconductors. Here integral dose of irradiation has general meaning; therefore in this case photochemical

ionizing processes give basic contribution and processes of radiated relaxation are neglected.

With including of light reflection data of Table 2 must be increased on 20-30 percents for regimes of irradiation the Nedimium laser (both regimes) and 250 percents for eximer laser irradiation (reflectance of eximer laser radiation is equaled 60 percents).

In addition we must remember that Ruby laser radiation for crystalline silicon has absorbance on order less as for amorphous, therefore for short regimes of irradiation the processes of bonds breakage may give more influence as for case of Nd-laser irradiation. Polycrystalline layer may include various crystalline phases. We can select condition of irradiation with creation on surface of silicon the nanostructures with various its fourth crystallographic modifications.

The role of irradiated atmosphere on formation of laser-induced surface nanostructures is shown in Fig. 1, Fig. 5 – Fig. 9. An oxidation processes are smooth out the surface (Fig. 1 and Fig. 5). The decreasing of oxygen concentration is caused the more intensive growth of microcolumns (Fig. 5, Fig. 6) and nanocolumns (Fig. 9).

The cascade model may be used for the explanation of experimental data of Fig. 10 – Fig. 13. Titanium has two phases: hexagonal and body-centered cubic. But after heating the titanium to 882,5°C it has only cubic phase [11]. According to cascade model peaks of proper surface columns must have hexagonal symmetry, but its generation is attended with oxidation processes. Therefore the intensities of creation the surface structures are various for two groups of pulses: for second group (70 – 110 pulses) is more intensive process as for first group of pulse (10 – 50 pulses). Among these regimes of irradiation may be receive the doubling of period of interference pattern (Fig. 13).

This method was used for the explanation of the experimental data about laser-induced transformations in various allotropic phases of carbon, included diamond, graphite, fullerenes and other [1] too.

Conclusions

1. The experimental data of creation surface laser-induced structures on silicon, germanium and titanium are discussed.
2. Possibility of using Chandrasekar-Haken-Ebeling model of Benar effect for explanation these data is analyzed: this model can't be used for the research the creation laser-induced hexagonal structures on germanium with diamond symmetry.
3. Cascade model of step-by-step excitation of proper chemical bonds in the regime of saturation the excitation is observed.
4. We show that cascade model allows explaining basic peculiarities of represented experimental data, including generation of new phases.

References

1. Trokhimchuck P. P. Relaxed Optics: Realities and Perspectives. –Saarbrücken: Lambert Academic Publishing, 2016. –250 p.
2. A. Medvid', "Nano-cones Formed on a Surface of Semiconductors by Laser Radiation: Technology Model and Properties," Nanowires Science and Technology, ed. Nicoletta Lupu, Inech, Vukovar, pp. 61–82, 2010.
3. Haken H. Synergetics. – H. Haken. Moscow: Mir, 1980. – 405 p. (In Russian).
4. Chandrasekar S. Hydrodynamic and Hydromagnetic Stability. – New York: Dover Publications, 1961. – 656 p.
5. Ebeling W. Creation structures under irreversible processes. – Moscow: Mir, Moscow, 1979. – 278 p. (In Russian).
6. Trokhimchuck P. P. Nonlinear Dynamical Processes. – Lutsk: Vezha-Print, 2015. – 280 p. (In Ukrainian).
7. Pedraza A. J., Fowlkes J. D., Lowndes D. H. Silicon microcolumn arrays growth by nanosecond pulse laser irradiation.// Appl. Phys. Lett., vol. 74, no. 10, 1999. – P. 2222-2224.
8. A. J. Pedraza, Y. F. Guan, J. D. Fowlkes, D. A. Smith and D. H. Lowndes, "Nanostructures produced by ultraviolet laser irradiation of silicon. I. Rippled structures," J. Vac. Sc. @ Techn. B., vol. 22, no. 10, pp. 2823-2835, 2004.
9. Tsukamoto M., Asuka K, Nakano N., Hashida M., Ratto M., Abe N., Fujita M. Period microstructures produced by femtosecond laser irradiation on titanium plate.// Vacuum, vol. 80, 2006. – P. 1346-1350.
10. Makin V. S. Peculiarities of the formation the ordered micro and nanjstructures in condensed matter after laser excitation of surface polaritons modes. D. Sc. (Physics and Mathematics) Thesis./ V. S. Makin. – Saint-Petersburg: State university of information technologies, mechanics and optics, 2013. – 384 p.
11. Donachie M. J. Titanium: A Technical Guide. – Ohio: Materials Park, 2000. – 380 p.
12. Birnbaum M. Semiconductor surface damage produced by Ruby Laser.// Journal of Applied Physics, vol. 36, Issue 11, 1965. – P. 3688–3689.
13. Shen M., Carey J. E., Crouch C. H., Kandyla M., Stone H. A. , Mazur E. High-density regular arrays of nanoscale rods formed on silicon surfaces via femtosecond laser irradiation in water. //Nanoletters, vol. 8, no.7, 2008. – P. 2087-2091.
14. Trokhimchuck P. P. Problems of reradiation and reabsorption in Relaxed Optics.// International Journal of Advanced Research in Physical Science (IJARPS). 2017. Vol. 4. № 2. P. 37 – 50.
15. Philips J.C. Metastable honeycomb model of laser annealing.//Journal of Applied Physics, No.12, Vol. 52, 1981. – P.7397–7402.
16. Tauc Ya. Optical properties of semiconductors in visible and ultraviolet ranges./Uspekhi fizicheskikh nauk, 1968, Vol. 94, Is. 3, P. 501 – 533. (In Russian)
17. Trokhimchuck P. P. Radiation physics of status solid./ P. P. Trokhimchuck. – Lutsk: Lesya Ukrayinka Volyn' National University Press "Vezha", 2007. – 394 p. (In Ukrainian).
18. Druzhynin A. , Ostrovskii I., Kogut Yu. Silicon and Germanium Whispers and its Solid Solutions in Sensor Electronics. – Lviv: National University "Lvivska polytehnika" Press, 2010. – 200 p. (In Ukrainian).